



1 **A translation wave model: Güneycedere case study**

2

3 **Hülya Çakır¹ and Mustafa Erol Keskin²**

4

5 **1. Graduate School of Natural and Applied Sciences, Süleyman Demirel University,**
6 **Isparta, 32260, Türkiye**

7

8 **2. Department of Civil Engineering, Süleyman Demirel University, Isparta, 32260,**
9 **Türkiye**

10

11 **Correspondence: Hülya Çakır (hulyacakir@dsi.gov.tr)**

12

13

14

15

16

17

18

19

20

21

22

23

24

25

26

27

28

29

30

31

32

33

34



35 **Abstract**

36 This study proposed a flood routing model which was derived from Saint-Venant (SV)
37 equations. It can be called translation wave model (TWM). In this model, bed slope term and
38 friction slope term were ignored in the momentum equation of SV equations. This means, the
39 difference between bed slope and friction slope are relatively small compared to other terms in
40 the SV equations. This approach is similar to the one in kinematic wave model (KWM), but in
41 KWM inertia and pressure terms are neglected. In this study, governing equations for the
42 proposed model were derived and solved numerically by using an explicit scheme. Then,
43 validation of the proposed model was obtained through real flood data that belong to an actual
44 creek reach in Isparta Province, Turkiye. The creek reach was between two stream gauging
45 stations and the inflow and outflow hydrographs of a real flood event were available. Also,
46 KWM was implemented for this creek reach using this real flood event. Thus two simulated
47 outflow hydrographs; one that belongs to KWM and another that belongs to TWM were created.
48 Then the two simulated outflow hydrographs were compared by differences in peak discharge,
49 time to peak flow and hydrograph volume. Since KWM fails to predict attenuation and
50 dispersion in outflow hydrographs, relative error of peak flow in KWM is calculated bigger
51 than in TWM (2,19% > -0,27%). Relative error of time to peak flow in TWM is calculated as
52 0,00% while it is calculated -2,50% in KWM and the two models failed to provide volume
53 conservation. Also, TWM and KWM were evaluated by the statistical parameters; Root Mean
54 Square Error (RMSE), Mean Absolute Error (MAE) and Nash-Sutcliffe Efficiency (NSE). The
55 results were in acceptable range but KWM gave better results since the creek reach had a steeper
56 slope than average ($S_0 \geq 0.005$). Finally, for comparison, an inflow hydrograph from literature
57 was routed with KWM and TWM in a rectangular channel.

58

59 **1 Introduction**

60

61 Flood or flow routing is a method to predict time and magnitude of flood/flow in a river or a
62 channel from available upstream inflow data. Flood routing is classified into two types;
63 hydrologic routing and hydraulic routing. In hydrologic routing, flow is only time dependent
64 while in hydraulic routing flow is space and time dependent (Chow et al., 1988). In hydrologic
65 routing; continuity equation and a relation between inflow, outflow and storage is used to solve
66 the routing problem. Solution process is relatively simple and results are satisfactory in general
67 (Shaw, 2005). In hydraulic routing topographical data is needed to solve complex equations
68 while in hydrologic routing there is less need of topographical data (Zhang et al., 2016).



69 In 1848 Barré de Saint-Venant first put forward a solution to hydraulic flood routing problem.
70 However, there is evidence in the literature that it was derived first by Lagrange as early as
71 1781 (Stoker, 1948). In the mentioned solution, “continuity equation” and a statement of
72 Newton's Second Law “momentum equation” are solved for a differential volume of one-
73 dimensional flow. In order to obtain an analytical solution, various approximations to the SV
74 equations have been proposed, because of difficulties in analytical solution of the complete
75 model, called a dynamic wave model. On the other hand, for many problems, a full solution of
76 the SV equations is unnecessary and a variety of simplified methods exist (Heatherman, 2008).
77 KWM is the simplest form of SV equations and it fails to predict attenuation and dispersion in
78 outflow hydrographs. This model is used when downstream backwater effect is insignificant
79 (Lighthill and Witham 1955a, 1955b). Another form of SV equations is diffusion wave model
80 (DWM). This model is not suitable for reaches that have dramatically varying cross sectional
81 areas and for very small slopes (Heatherman, 2008). In this study another simplified form of
82 SV equations is proposed. It can be called TWM. This model can be considered as a
83 nonkinematic model because of its neglected terms in SV equations. Since KWM is suitable
84 for steep slopes (Henderson, 1966), TWM can be suitable for mild slopes.

85

86 In this study, firstly basic equations of TWM were derived. Secondly, numerical solution of the
87 model was described. Then applicability of the model was studied by routing an observed
88 inflow hydrograph for a creek reach length of 1764 m with a trapezoidal shape in general. The
89 creek reach was between two gauging stations and was in Isparta province of Turkiye. Also
90 equations of KWM were given in this study and the observed inflow hydrograph was routed by
91 KWM in HEC-HMS. Results of the two model were compared with the observed outflow
92 hydrograph.

93

94 **2 Study site and data**

95

96 **2.1 Study site**

97

98 Güneycedere Creek is in Isparta Province of Turkiye. Catchment area of Güneycedere Creek
99 basin covers 102 km². Study area is located in lower reach of this creek. The creek flows
100 northwesterly toward Lake Eğirdir which is also known as the “Seven Colored Lake” in Isparta.

101

102 There are several reasons to choose this creek reach for this study:



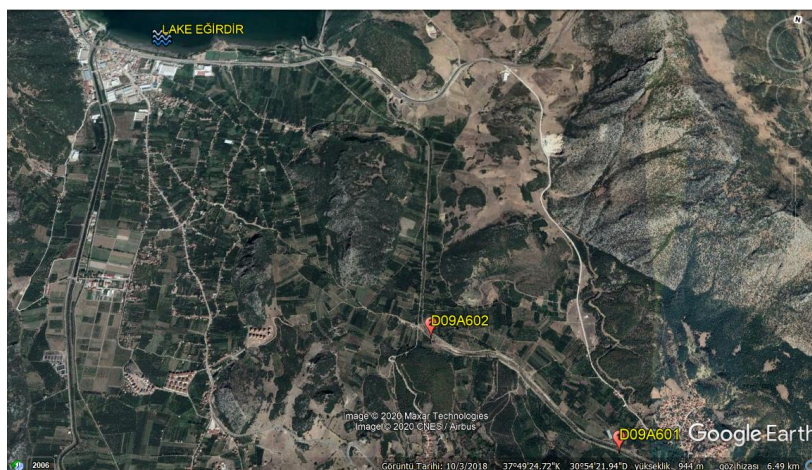
103 . In the study area, there are two stream gauging stations. Thus, observed inflow hydrograph
104 and observed outflow hydrograph are available. Distance between upper gauging station
105 (D09A601) and lower gauging station (D09A602) is 1764 metres in length (Fig. 1, Fig. , 2. and
106 Fig. 3).

107 . There is no lateral inflow or outflow between the stations along the creek reach.

108 . There is no abrupt changes in the cross sectional areas along creek the reach.

109 . Slope of the creek reach is relatively a mild slope when compared to other creeks that have
110 gauging stations.

111



112

113

114

Figure 1 Study area © Google Earth 2018



115

116

Figure 2 Stream gauging station D09A601



117

118

Figure 3 Stream gauging station D09A602

119

120 2.2 Data

121

122 The inflow hydrograph and the outflow hydrograph chosen for this study belong to flood event
123 occurred in 2018 spring. The two hydrographs have good hydrograph shapes. Base flow of the
124 creek reach is assumed to be the minimum flow in the inflow hydrograph and is $7.19 \text{ m}^3/\text{s}$.
125 Elapsed time of the two hydrographs is 9 hours. They have single peak flows. Time to peak
126 flow in the inflow hydrograph is 3 hours and lag of time to peak in the outflow hydrograph is
127 0.33 hours.

128

129 In this study, a 1:1000 scale digital topographical map of the study area was used. Based on the
130 topographical map, bed slope between upper and lower gauging stations was calculated as
131 0.006236. The value of Manning roughness coefficient (n) was derived from the well-known
132 Manning equation. “ n ” roughness coefficient was the average value for the whole reach and it
133 was calculated as 0.037. Since the creek bed is lined with gravels and stones, the calibrated
134 value of “ n ” is compatible with “Manning roughness coefficients for various open channel
135 surfaces” (Chow et al., 1988).

136

137

138

139



140 **3 Methodology**

141

142 **3.1 Governing equations**

143

144 SV equations solve both the continuity and momentum equations for a differential volume of
145 one-dimensional flow, where the forces on the control volume are limited to the effect of
146 gravity, pressure variation, and friction or roughness of the channel walls. Mass is conserved in
147 the solution and the effect of acceleration within the control volume and momentum flux across
148 the upstream and downstream faces are considered (Heatherman, 2008).

149

150 Neglecting wind shear and eddy losses, the continuity equation is stated as:

151

152
$$\frac{\partial A}{\partial t} + \frac{\partial Q}{\partial x} = 0 \quad (1)$$

153

154 where A is cross-sectional area of flow, t is time, Q is discharge and x is longitudinal distance
155 of the control volume. The continuity equation is same for all forms of SV equations.

156

157 The momentum equation can be stated as:

158

159
$$a \left[\frac{\partial Q}{\partial t} + \frac{\partial \left(\frac{Q^2}{A} \right)}{\partial x} \right] + b \left[gA \frac{\partial y}{\partial x} \right] + c \left[gA (S_0 - S_f) \right] = 0 \quad (2)$$

160 term1 term2 term3 term4 term5

161

162 where g is gravitational acceleration, y is depth of flow, S₀ is bed slope and S_f is frictional slope.

163

164 In Equation 2, term 1 arises from temporal acceleration, term 2 from convective acceleration,
165 term 3 from net pressure forces on the control volume, term 4 from gravitation force and term
166 5 from friction force.

167



168 In the momentum equation (Eq. 2), if $a=1$, $b=1$, and $c=1$, then momentum equation of the
169 dynamic wave model is obtained. If $a=0$, $b=1$, and $c=1$, then momentum equation of the
170 diffusion wave model is obtained.

171

172 3.1.1 KWM

173

174 In the momentum equation (Eq. 2) if $a=0$, $b=0$, and $c=1$, then momentum equation of the
175 kinematic wave model is obtained in Eq. (3).

176

$$177 S_o = S_f \quad (3)$$

178

179 which means that the flow is uniform and a function of depth or channel's average cross-
180 sectional area.

181

182 The momentum equation of KWM can be written as:

183

$$184 Q = \alpha A^\beta \quad (4)$$

185

186 where α and β are the kinematic wave model parameters. Substituting Eq. (4), in Eq. (1) yields
187 an expression for solving for Q as the only dependent variable (Chow et al., 1988):

188

$$189 \frac{\partial Q}{\partial x} + \alpha \beta Q^{\beta-1} \left(\frac{\partial Q}{\partial t} \right) = 0 \quad (5)$$

190

191 3.1.2 TWM

192

193 In Equation 2, if $a=1$, $b=1$, and $c=0$, then momentum equation of TWM is obtained:

194

$$195 \frac{\partial Q}{\partial t} + \frac{\partial \left(\frac{Q^2}{A} \right)}{\partial x} + gA \frac{\partial y}{\partial x} = 0 \quad (6)$$

196



197 In the momentum equation of TWM, inertia and pressure terms are included while gravitation
198 and friction terms are neglected. This model can be considered as a nonkinematic model. Since
199 kinematic wave model is suitable for steep slopes, TWM can be suitable for mild slopes.

200

201 For a trapezoidal channel, the cross-sectional area of the channel is given by:

202

$$203 \quad A = (B + zy) y \quad (7)$$

204

205 where B is bottom width and z is the inverse of the side slope of the channel. In Equation (7)
206 $z=0$ for rectangular channels, and $B=0$ for triangular channels.

207

208 Using Eq. (7), if B is constant the partial derivative can be written as:

209

$$210 \quad \frac{\partial A}{\partial x} = T \frac{\partial y}{\partial x} \quad (8)$$

211

212 where $T = B + 2zy$ as width of water surface.

213

214 Substituting Eq. (8) into Eq. (6), Eq. (9) is achieved:

215

$$216 \quad \frac{\partial Q}{\partial t} + \frac{\partial \left(\frac{Q^2}{A} \right)}{\partial x} + gA \frac{1}{T} \frac{\partial A}{\partial x} = 0 \quad (9)$$

217

218 Equation (9) can be rearranged as:

219

$$220 \quad \frac{\partial Q}{\partial t} + \frac{1}{A} 2Q \frac{\partial Q}{\partial x} - \frac{Q^2}{A^2} \frac{\partial A}{\partial x} + \frac{gA}{T} \frac{\partial A}{\partial x} = 0 \quad (10)$$

221

222 Multiplying both sides with A^2 , Eq. (10) becomes:

223

$$224 \quad A^2 \frac{\partial Q}{\partial t} + 2QA \frac{\partial Q}{\partial x} - Q^2 \frac{\partial A}{\partial x} + \frac{gA^3}{T} \frac{\partial A}{\partial x} = 0 \quad (11)$$

225



226 Equation (11) can be rearranged as:

227

$$228 \quad A^2 \frac{\partial Q}{\partial t} + 2QA \frac{\partial Q}{\partial x} + \left[\frac{gA^3}{T} - Q^2 \right] \frac{\partial A}{\partial x} = 0 \quad (12)$$

229

230 Equation (12) can be rewritten as:

231

$$232 \quad \alpha \frac{\partial Q}{\partial t} + \beta \frac{\partial Q}{\partial x} + \gamma \frac{\partial A}{\partial x} = 0 \quad (13)$$

233

234 where:

235

$$236 \quad \alpha = A^2 \quad (14)$$

237

$$238 \quad \beta = 2QA \quad (15)$$

239

$$240 \quad \gamma = \left(gA^3 / T \right) - Q^2 \quad (16)$$

241

242 In definition, $T = B + 2zy$ for trapezoidal channels, $T = B$ ($z = 0$) for rectangular channels, and $T =$
243 $2zy$ for triangular channels.

244

245 Equation (1) and Eq. (13) can be solved by using initial and boundary conditions. For a
246 triangular inflow hydrograph, the initial conditions can be written as:

247

$$248 \quad Q(x,0) = Q_0 \quad (17)$$

249

$$250 \quad A(x,0) = A_0 \quad (18)$$

251

252 Where Q_0 is the base constant flow, and A_0 is cross-sectional area corresponding to the base
253 flow.

254

255 The upstream boundary condition can be written as for $0 < t < t_p$:

256



257
$$Q(0, t) = Q_0 + \left(\frac{Q_p - Q_0}{t_p} \right) t \quad (19)$$

258

259 where Q_p is peak flow and t_p is time to peak.

260

261 For $t_p < t < t_b$ the upstream boundary condition is defined as:

262

263
$$Q(0, t) = Q_p - \left(\frac{Q_p - Q_0}{t_b - t_p} \right) t \quad (20)$$

264

265 Where t_b is duration of the inflow hydrograph.

266

267 Finally at the end of the inflow hydrograph the boundary condition becomes for $t > t_b$:

268

269
$$Q(0, t) = Q_0 \quad (21)$$

270

271 3.2 Numerical solution

272

273 In order to solve the governing equations of the model, an explicit difference method is used
274 (Abbot and Basco, 1989). Applying this finite difference method, as backwards in space and
275 forward in time, Equation (13) and Eq. (1) can be written respectively as follows:

276

277
$$Q_i^{j+1} = Q_i^j - \Delta t \left(\beta_i^j (Q_i^j - Q_{i-1}^j) + \gamma_i^j (A_i^j - A_{i-1}^j) \right) / ((\Delta x) \alpha_i^j) \quad (22)$$

278

279
$$A_i^{j+1} = A_i^j - \Delta t (Q_i^{j+1} - Q_{i-1}^{j+1}) / \Delta x \quad (23)$$

280

281 where Δx ve Δt are space and time intervals, respectively.

282

283 In the calculation procedure, first each pair of α_i^j , β_i^j and γ_i^j values can be readily calculated
284 from Eq. (14), Eq. (15) and Eq. (16) using the known initial and boundary data at starting point
285 of (i, j), then one can obtain Q_i^{j+1} from Eq. (22). Finally using Q_i^{j+1} , A_i^{j+1} can be calculated from
286 Eq. (23). This technique will be repeated for successive values of (i, j). In the procedure,



287 discharge that is leaving the downstream boundary of a channel segment, enters to the upstream
288 boundary of the next segment and establishes the upstream boundary condition for flow on this
289 next segment.

290

291 **3.3 Application**

292

293 In this study, applicability of the TWM is investigated in a gauged creek reach. In addition,
294 KWM is applied to this reach and the results of the two model are compared with the observed
295 data.

296

297 Also for comparison, some data were selected from literature (Akan and Yen, 1981). In order
298 to use the TWM, a rectangular channel with a width of 5 m is used. The initial values of the A,
299 corresponding to inflow hydrograph values were calculated by using Manning equation. For
300 given values of Q , n , S_0 and B (5 m); water depth and consequently A can be found by trial
301 and error method.

302

303 **3.3.1 Güneycedere Creek application**

304

305 All of the required physical components to perform KWM in HEC-HMS are calculated based
306 on the available flow and topographical data.

307

308 In Figure 4, length is the distance between upper and lower gauging stations and it is 1764
309 meters. Slope is the average bed slope between the two stations and it was calculated as
310 0.006236. “ n ” roughness coefficient is the average value for the whole reach and it was
311 calculated as 0.037. Bottom width is the average width of the bottom through the reach. In 2000,
312 a bank protection project was constructed within the lower basin of Güneycedere Creek
313 including the study area. The project consists of grading the Güneycedere Creek bank to a
314 2V:5H slope along 2500 meters of the eroded bank, and it is made of riprap (Fig. 2. and Fig.
315 3.). However, according to the cross section views created by Netcad computer program in the
316 creek reach, side slope was taken as 1V:3H in average.

317



Basin Name: CAYDERE	
Element Name: CAYDERE	
Initial Type:	Discharge = Inflow
*Length (M)	1764
*Slope (M/M)	0.006236
*Manning's n:	0.037
*Subreaches:	2
Index Method:	Flow
*Index Flow (M3/S)	
Shape:	Trapezoid
*Bottom Width (M)	15
*Side Slope (xH:1V)	3
Invert (M)	

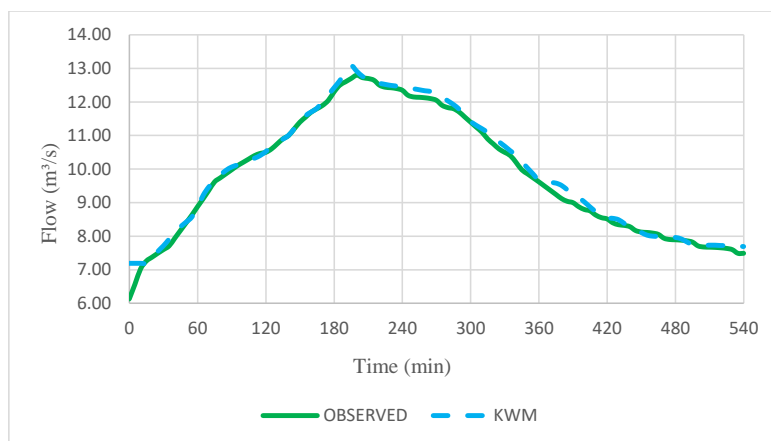
318

319

Figure 4 © HEC-HMS component editor for KWM

320

321 The peak flow in the inflow hydrograph of upstream gauging station D09A601 is $13,10 \text{ m}^3/\text{s}$.
322 After routing the inflow hydrograph with KWM in HEC-HMS, the outflow hydrograph is
323 computed. This simulated outflow hydrograph belongs to the downstream gauging station
324 D09A602 and the peak flow in the outflow hydrograph is computed as $13,08 \text{ m}^3/\text{s}$. Observed
325 peak outflow in the downstream gauging station D09A602 is $12,80 \text{ m}^3/\text{s}$. Time to peak flow in
326 the simulated outflow hydrograph is 15 minutes, while time to peak flow in the observed
327 outflow hydrograph is 20 minutes. Observed total outflow volume is 319.509 m^3 while
328 computed total outflow volume with KWM is 322.845 m^3 . In Figure 5, observed outflow
329 hydrograph and KWM's simulated hydrograph are given.



330

331

Figure 5 Observed outflow hydrograph and outflow hydrograph with KWM

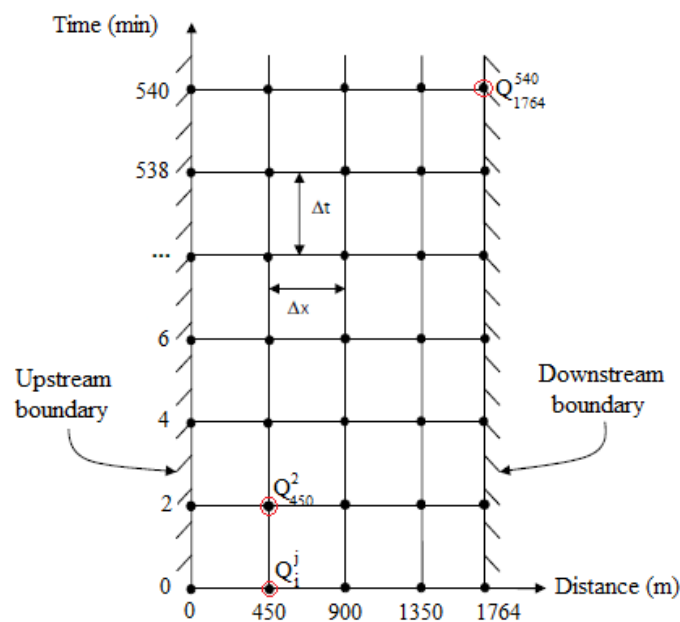


332 The TWM calculations are performed on a grid placed over x-t plane. The x-t grid is a network
333 of points defined by taking distance increments of length Δx and time increments of duration
334 Δt (Chow et al.,1988). On our x-t grid, upstream boundary condition on time line is composed
335 of the inflow hydrograph. This inflow hydrograph belongs to the upstream gauging station
336 D09A601. Initial boundary condition on the distance line is composed of base flow. As
337 mentioned before, base flow of the creek reach is assumed to be the minimum flow in the inflow
338 hydrograph and is $7.19 \text{ m}^3/\text{s}$.

339

340 In order to satisfy the courant condition as $c\Delta t < \Delta x$, in which c is the wave celerity, Δx and Δt
341 were set equal to various values and then for various values, TWM was applied to the creek
342 reach and it was seen that when $\Delta x = 450 \text{ m}$ and $\Delta t = 120 \text{ s}$, computational stability was
343 maintained and courant condition was satisfied. TWM x-t grid is given in Fig. 6.

344



345

346

Figure 6 Güneycedere TWM grid on an x-t plane

347

348 Starting from the upper gauging station, distance of the station' s location was assumed to be
349 KM:0+000 and was assumed to be the first point, labeled as number 1. Moving downstream



350 and considering “ $\Delta x = 450$ m”, other locations are specified along the 1764 metres long creek
351 reach respectively; 0+450 km (2), 0+900 km (3), 1+350 km (4) and 1+764 km (5). At these
352 points of the reach, cross section views were created in Netcad computer program. On the TWM
353 grid, distance points were denoted by index i and time points were denoted by index j .

354

355 Applying the finite difference method, as backwards in space and forward in time and using
356 Eq. (22), Q_i^{j+1} (Q_{450}^2) was calculated. Then Q_i^{j+2} (Q_{450}^4), Q_i^{j+3} (Q_{450}^6), Q_i^{j+4} (Q_{450}^8), ..., and Q_i^{j+n}
357 (Q_{450}^{540}) were calculated in the same way. While calculated flows formed the discharges that were
358 leaving the first segment of the creek reach they also formed the upstream boundary condition
359 for the next segment. In this way, the flows that belonged to the last point on the x - t grid were
360 calculated. This point represents the location of the downstream gauging station in the reach
361 and calculated flows of this point form the outflow hydrograph.

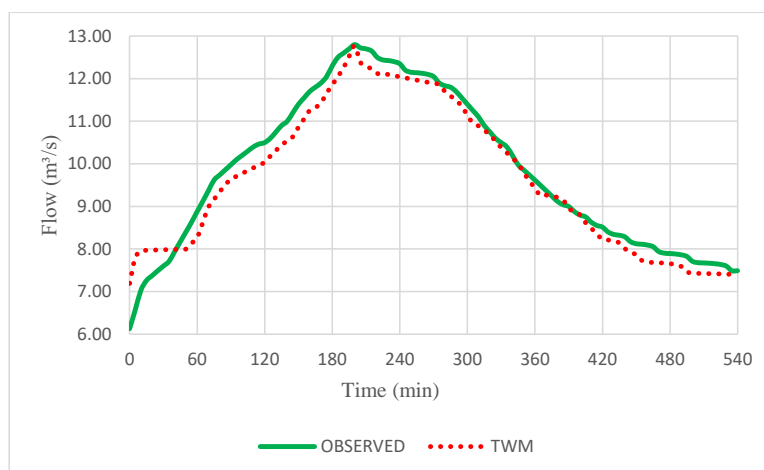
362

363 In rectangular, trapezoidal and triangular channels, Eq. (23) enables to do calculations without
364 the need of creating cross section views on each points on the x - t grid. Since this study was on
365 a natural creek and since the 1:1000 scale digital topographical map of the study area was
366 available, cross section views were created at each point by Netcad computer program easily.
367 For various water depths corresponding to various discharges in the cross sections; α_i^j , β_i^j and
368 γ_i^j were calculated using macros created in excel specific for this study.

369

370 The peak flow in the inflow hydrograph of upstream gauging station D09A601 is 13,10 m³/s.
371 After routing the inflow hydrograph with TWM, the outflow hydrograph is computed. This
372 simulated outflow hydrograph belongs to the downstream gauging station D09A602 and the
373 peak flow in the outflow hydrograph is computed as 12,77 m³/s. Observed peak outflow in the
374 downstream gauging station D09A602 is 12,80 m³/s. Time to peak flow in the simulated
375 outflow hydrograph is 200 minutes. This value is equal to the one in the observed outflow
376 hydrograph. Observed total outflow volume is 319.509 m³ while computed total outflow
377 volume with TWM is 312.990 m³. In Figure 7, observed outflow hydrograph and TWM' s
378 simulated hydrograph are given.

379



380

381

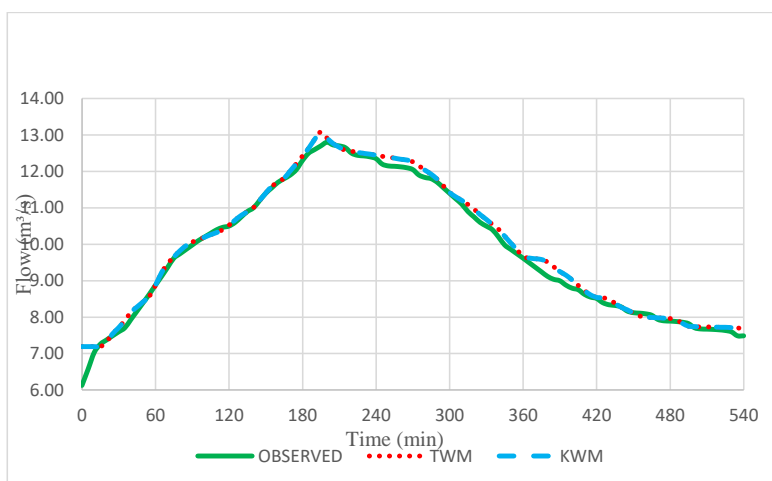
Figure 7 Observed outflow hydrograph and outflow hydrograph with TWM

382

383 Observed outflow hydrograph and outflow hydrographs with TWM and KWM are given in Fig.

384 8.

385



386

387

Figure 8 Observed outflow hydrograph and outflow hydrographs with TWM and KWM

388

389 3.3.2 Application of KWM and TWM with literature data

390

391 As an example of the application of the KWM in HEC-HMS, it was applied to a rectangular
392 channel with a width of 5 m and a bottom slope of 0.005, and the Manning roughness coefficient
393 of 0.012. Reach length (L) of the channel was assumed to be 1000 m. In the inflow hydrograph



394 peak flow is $12.00 \text{ m}^3/\text{s}$, baseflow is $3.00 \text{ m}^3/\text{s}$. Elapsed time of the inflow hydrograph is 2400
395 s (40 min) and time to peak flow is 600 s (10 min).

396

397 After routing the inflow hydrograph with KWM in HEC-HMS, the outflow hydrograph is
398 computed. The peak flow in the simulated outflow hydrograph is computed as $11.55 \text{ m}^3/\text{s}$. Time
399 to peak flow in the simulated outflow hydrograph is 14 min.

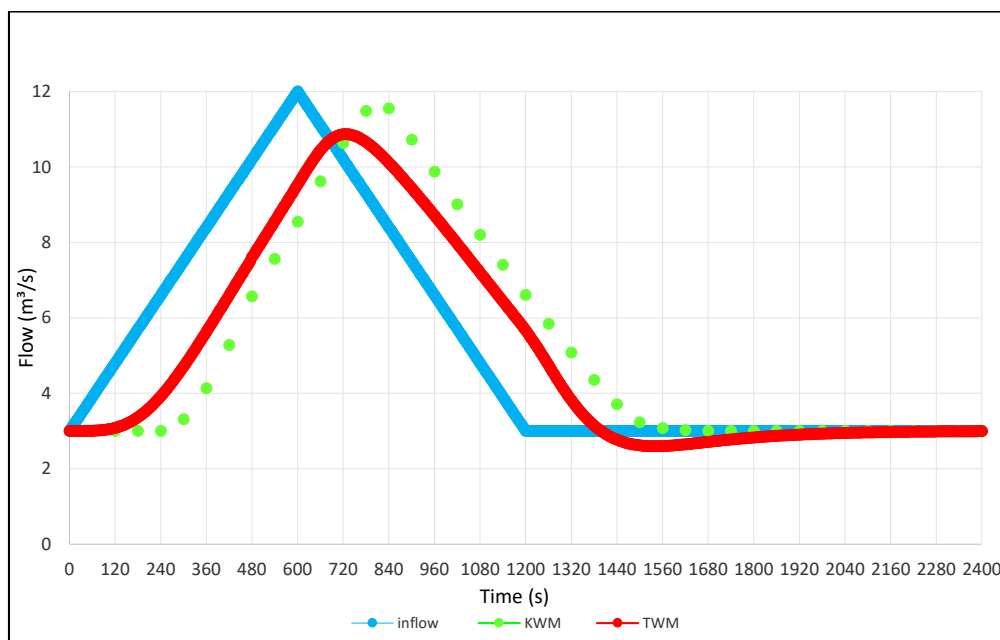
400

401 Using the same data (inflow hydrograph, n , S_0 , L and B), TWM was applied to the rectangular
402 channel. In order to satisfy the Courant condition, $\Delta x = 200 \text{ m}$ and $\Delta t = 5 \text{ s}$ were used in the
403 computations. After routing the inflow hydrograph with TWM, the outflow hydrograph is
404 computed. The peak flow in the simulated outflow hydrograph is computed as $10.9 \text{ m}^3/\text{s}$. Time
405 to peak flow in the simulated outflow hydrograph is 12.08 min.

406

407 Inflow hydrograph and simulated outflow hydrographs are given in Fig. 9.

408



409

410 Figure 9 Inflow hydrograph (Akan and Yen, 1981) and simulated outflow hydrographs

411

412

413



414 **3.4 Statistical analyses**

415

416 Since observed inflow and observed outflow hydrographs in Güneycedere Creek reach were
 417 available in this study, we could be able to compare the simulated KWM and TWM
 418 hydrographs with the observed outflow hydrograph. Above, in Fig. 8, it was clear that the
 419 simulated KWM and TWM hydrographs had good agreement with the observed outflow
 420 hydrograph. Although visual comparison of the observed and simulated outflow hydrographs
 421 gave a positive opinion about the accuracy of the KWM and TWM in the study area, statistical
 422 analyses were needed to support this opinion. The root-mean-square error (RMSE) in Eq. (24),
 423 the mean absolute error (MAE) in Eq. (25) and the Nash–Sutcliffe model efficiency coefficient
 424 (E) in Eq. (26) were calculated to determine the difference between the observed and simulated
 425 hydrographs.

426

427
$$RMSE = \sqrt{\frac{\sum_{i=1}^n (Q_c - Q_o)^2}{n}} \quad i=1, 2, 3, \dots, n \quad (24)$$

428
$$MAE = \frac{\sum_{i=1}^n |Q_c - Q_o|}{n} \quad i=1, 2, 3, \dots, n \quad (25)$$

429
$$E = \frac{\sum_{i=1}^n (Q_o - Q_{mo})^2 - \sum_{i=1}^n (Q_o - Q_c)^2}{\sum_{i=1}^n (Q_o - Q_{mo})^2} \quad i=1, 2, 3, \dots, n \quad (26)$$

430

431 RMSE, MAE and E values were given in Table 1.

432

433 Table 1 RMSE, MAE and NSE values

Model	RMSE (m ³ /s)	MAE (m ³ /s)	NSE
TWM	0,36	0,30	0,96
KWM	0,18	0,12	0,99

434

435 Relative errors of 1) peak flow, 2) time to peak and 3) volume are computed as shown in Eq.
 436 (27), Eq. (28) and Eq. (29).

437



$$438 \quad \sigma_{\text{peak}} = \left(\frac{Q_{pc}}{Q_{po}} - 1 \right) 100 \quad (27)$$

$$439 \quad \sigma_{\text{time}} = \left(\frac{t_{pc}}{t_{po}} - 1 \right) 100 \quad (28)$$

$$440 \quad \sigma_{\text{volume}} = \left(\frac{V_c}{V_o} - 1 \right) 100 \quad (29)$$

441 where:

442 Q_c = Computed flows in the outflow hydrograph (m^3/s)

443 Q_o = Observed flows in the outflow hydrograph (m^3/s)

444 σ_{peak} = Relative error of peak flow (%)

445 Q_{pc} = Computed peak outflow (m^3/s)

446 Q_{po} = Observed peak outflow (m^3/s)

447 σ_{time} = Relative error of time to peak flow (%)

448 t_{pc} = time to peak flow in the computed outflow hydrograph (h)

449 t_{po} = time to peak flow in the observed outflow hydrograph (h)

450 σ_{volume} = Relative error of total volume (%)

451 V_c = Total volume of the the computed hydrograph (m^3)

452 V_o = Total volume of the the observed hydrograph (m^3)

453 Q_{mo} = Mean of the observed outflows (m^3/s)

454

455 σ_{peak} , σ_{time} and σ_{volume} values were given in Table 2.

456

457 Table 2 Relative errors of peak flow, time to peak and volume

Model	Q_{gp} (m^3/s)	Q_{hp} (m^3/s)	σ_p (%)	t_{gp} (saat)	t_{hp} (saat)	σ_t (%)	V_g (m^3)	V_h (m^3)	σ_v (%)
TWM	12,80	12,77	-0,27	3,33	3,33	0,00	319509	312990	-2,04
KWM	12,80	13,08	2,19	3,33	3,25	-2,50	319509	322845	1,04

458

459 4. Discussion and conclusions

460

461 At the end of this study, the following concluding points can be made:

462

463 1. In this study, a translation wave model (TWM) was developed for a trapezoidal channel. This
 464 model was adapted to simulate the outflow hydrograph in a gauged creek reach and also to



465 predict the outflow hydrograph in a rectangular channel that was a special case of a trapezoidal
466 channel.

467

468 2. The results of the TWM were compared with those of the KWM. TWM was successfully
469 applied in Güneycedere Creek in terms of peak flow (PF) and time to peak flow (TPF). In other
470 words, KWM gave a value that was bigger than the observed value in terms of PF, but, TWM
471 gave a very close value to observed value. TWM gave the exact value to the observed value in
472 terms TPF, but, KWM gave a close value to observed one. KWM results supports the fact that
473 there is no attenuation and dispersion in outflow hydrographs when they are simulated by
474 KWM.

475

476 2. Relative error of volume (REV) in TWM was in the form of decreasing of volume while
477 REV in KWM was in the form of increasing of volume.

478

479 3. According to the statistical analyses that were performed in this study, KWM gave better
480 results than TWM. Bed slope of the creek reach that was subject to this study was approximately
481 0,006 ($\geq 0,005$) and it was a steep slope (Soentoro, 1991). KWM' s momentum equation was
482 composed of bed slope and friction slope terms and KWM was suitable for steep slopes. In the
483 momentum equation of TWM bed slope term and friction slope term were neglected. Thus
484 TWM was more accurate to use in smooth sloped river reaches. Statistical analyses' results
485 supported this conclusion.

486

487 4. In addition, for comparison, an inflow hydrograph from literature was routed with KWM and
488 TWM in a rectangular channel. As expected, in the KWM' s simulated hydrograph the peak
489 flow was calculated as a very close value to the peak flow in the inflow hydrograph. In the
490 TWM' s simulated hydrograph, the peak flow was calculated in an acceptable value ranges and
491 the simulated hydrograph had a good shape.

492

493 As a result, TWM' s momentum equation does not include the friction and bed slope. This
494 implies that the numerical solution of this model can be more stable and takes less time than
495 that of any other model that includes these terms. TWM needs only one boundary condition. So
496 this model can be solved for supercritical flows.

497

498



499 **Author contributions**

500

501 HÇ and MEK developed the model, HÇ collected hydrological and survey data, performed the
502 analysis and wrote the manuscript. MEK supervised and improved the study.

503

504 **Competing interests**

505 The authors declare that they have no conflicts of interest.

506

507

508

509

510

511

512

513

514

515

516

517

518

519

520

521

522

523

524

525

526

527

528

529

530

531

532



533 **References**

534

535 Abbott, M.B. and Basco, D.R.: Computational Fluid Dynamics, Longman Group UK Limited,
536 UK, 1989.

537

538 Akan, A.O., and Yen, B.C.: Diffusion-wave flood routing in channel networks, J. Hydraul. Div.,
539 Am. Soc. Civ. Eng., 107(6), 719– 732, 1981.

540

541 Chow, V.T., Maidment, D.R., Mays, L.W.: Applied Hydrology, McGraw-Hill Inc, USA, 1988.

542 Heatherman, W.J.: Flood Routing on Small Streams: A Review of Muskingum-Cunge,
543 Cascading Reservoirs and Full Dynamic Solutions. Ph.D. thesis, University of Kansas, USA,
544 351 pp., <http://hdl.handle.net/1808/4349>, 2008.

545

546 Henderson, F.M.: Open Channel Flow, Macmillan, 522 pp, 1966.

547

548 Lighthill, M.J., and Witham, G.B.: On kinematic waves I: Flood movement in long rivers, Proc.
549 R. Soc. London, Ser. A, 229, 281 –316, <https://doi.org/10.1098/rspa.1955.0088>, 1955a.

550

551 Lighthill, M.J., and Witham, G.B.: On kinematic waves II: A theory of traffic flow on long
552 crowded roads, Proc. R. Soc. London, Ser. A, 229, 317 – 345,
553 <https://doi.org/10.1098/rspa.1955.0089>, 1955b.

554

555 Shaw, E.M.: Hydrology in Practice, Taylor&Francis Group, USA, 2005.

556 Soentoro, E.A.: Comparison of Flood Routing Methods, M.Sc. thesis, University of British
557 Columbia, 106p, Canada, <https://doi.org/10.14288/1.0050451>, 1991.

558

559 Stoker, J.J.: The formation of breakers and bores: The theory of nonlinear wave propagation in
560 shallow water and open channels, Communications on Applied Mathematics, Vol. I, No. 1, 1-
561 87, <https://doi.org/10.1002/cpa.3160010101>, 1948.

562

563 Zhang, S., Kang, L., Zhou, L., Guo, X.: A new modified nonlinear Muskingum model and its
564 parameter estimation using the adaptive genetic algorithm, Hydrology Research, 48(1):17-27,
565 <http://dx.doi.org/10.2166/nh.2016.185>, 2016.